High-power parametric conversion from near-infrared to short-wave infrared

Adrien Billat,[1,*] Steevy Cordette,[1] Yu-Pei Tseng,[1] Svyatoslav Kharitonov[1] and Camille-Sophie Brès[1]

[1]Photonic Systems Laboratory, Ecole Polytechnique Fédérale de Lausanne (EPFL) STI IEL, CH-1015. Lausanne, Switzerland

[*]adrien.billat@epfl.ch

Abstract: We report the design of an all-fiber continuous wave Short-Wave Infrared source capable to output up to 700 mW of power at 1940 nm. The source is tunable over wavelength intervals comprised between 1850 nm and 2070 nm depending on its configuration. The output can be single or multimode while the optical signal to noise ratio ranges from 25 and 40 dB. The architecture is based on the integrated association of a fiber optical parametric amplifier and a Thulium doped fiber amplifier.

OCIS codes: (190.4975) Parametric processes; (230.2285) Fiber devices and optical amplifiers; (060.4370) Nonlinear optics, fibers; (140.3070) Infrared and far-infrared lasers.

References and links

1. M. N. Petrovich, F. Poletti, J. P. Wooler, A.M. Heidt, N.K. Baddela, Z. Li, D.R. Gray, R. Slavík, F. Parmigiani, N.V. Wheeler, J.R. Hayes, E. Numkam, L. Grűner-Nielsen, B. Pálsdóttir, R. Phelan, B. Kelly, John O'Carroll, M. Becker, N. MacSuibhne, J. Zhao, F.C. Garcia Gunning, A.D. Ellis, P. Petropoulos, S.U. Alam, and D. J. Richardson, "Demonstration of amplified data transmission at 2 μm in a low-loss wide bandwidth hollow core photonic bandgap fiber," Opt. Express **21**, 28559–28569 (2013).
2. S. D. Jackson, "Towards high-power mid-infrared emission from a fibre laser," Nature Photon. **6**, 423-431 (2012).
3. Z. Li, S. U. Alam, Y. Jung, A. M. Heidt, and D. J. Richardson, "All-fiber, ultra-wideband tunable laser at 2 μm," Opt. Lett. **38**, 4739–4742 (2013).
4. N. Simakov, A. Hemming, W. A. Clarkson, J. Haub, and A. Carter, "A cladding-pumped, tunable holmium doped fiber laser," Opt. Express **21**, 28415-28422 (2013).
5. B. P.-P. Kuo, M. Hirano, and S. Radic, "Continuous-wave, short-wavelength infrared mixer using dispersion-stabilized highly-nonlinear fiber," Opt. Express **20**, 18422-18431 (2012).
6. F. Gholami, B. P.-P. Kuo, S. Zlatanovic, N. Alic, and S. Radic, "Phase-preserving parametric wavelength conversion to SWIR band in highly nonlinear dispersion stabilized fiber," Opt. Express **21**, 11415-11424 (2013).
7. J. M. Chavez Boggio, S. Moro, B. P.-P. Kuo, N. Alic, B. Stossel, and S. Radic, "Tunable Parametric All-Fiber Short-Wavelength IR Transmitter," J. Lightw. Technol. **28**, 443-447 (2010).
8. A. Gershikov, J. Lasri, Z. Sacks, and G. Eisenstein, "A tunable fiber parametric oscillator for the 2 μm wavelength range employing an intra-cavity thulium doped fiber active filter," Opt. Commun. **284**, 5218-5220 (2011).
9. B. Auguie. A. Mussot, A. Boucon, E. Lantz, and T. Sylvestre, "Ultralow chromatic dispersion measurement of optical fibers with a tunable fiber laser," IEEE Photon. Technol. Lett. **18**, 1825-1827 (2006).
10. M. E. Marhic, K. K.-Y. Wong, and L. G. Kazovsky, "Wide-band tuning of the gain spectra of one-pump fiber optical parametric amplifiers," IEEE J. Sel. Topics Quantum Electron. **10**, 1133-1141 (2004).
11. S. D. Agger, and J. H. Povlsen, "Emission and absorption cross section of thulium doped silica fibers," Opt. Express **14**, 50-57 (2006).
12. J. Lee, U.-C. Ryu, A, S. Joon, and N. Park, "Enhancement of power conversion efficiency for an L-band EDFA with a secondary pumping effect in the unpumped EDF section," IEEE Photon. Technol. Lett. **11**, 42-44 (1999).
13. Z. Li, A. M. Heidt, J. M. O. Daniel, Y. Jung, S. U. Alam, and D. J. Richardson, "Thulium-doped fiber amplifier for optical communications at 2 μm," Opt. Express **21**, 9289-9297 (2013).
14. B. P.-P. Kuo, and S. Radic, "Highly nonlinear fiber with dispersive characteristic invariant to fabrication fluctuations," Opt. Express **20**, 7716-7725 (2012).
15. M. Farahmand, and M. de Sterke, "Parametric amplification in presence of dispersion fluctuations," Opt. Express **12**, 136-142 (2004).

16. A. Willinger, E. Shumakher and G. Eisenstein, "On the Roles of Polarization and Raman-Assisted Phase Matching in Narrowband Fiber Parametric Amplifiers," J. Lightw. Technol. **26**, 2260-2268 (2008).
17. F. Gholami, S. Zlatanovic, E. Myslivets, S. Moro, B. Kuo, C. Brès, A. Widberg, N. Alic and S. Radic, "10Gbps Parametric Short-Wave Infrared Transmitter," in Optical Fiber Communication Conference, OSA Technical Digest (CD) (Optical Society of America, 2011), paper OThC6.

1. Introduction

The 2 µm spectral region has gathered significant interest during the past years as these wavelengths are well suited for hollow core fiber communication [1], gas sensing or non-linear generation [2]. Most of these applications would highly benefit from an easily tunable, energy efficient and modulation capable source. Short wave infrared (SWIR) fiber sources based on classical fiber laser architectures have recently been demonstrated [3]. It has however proven difficult to reach high levels of power while operating in the continuous wave (CW) regime, except with bulky configurations mixing fiber and free-space optics [4]. Alternative schemes based on parametric conversion in silica fibers have been reported these past years [5, 6]. While these schemes are more versatile, the maximum obtainable CW power remained below -10 dBm, with conversion efficiency (CE, idler power at the output divided by the signal power at the input) reaching -15 dB. With a pulsed regime pumping, which implies the generation of pulsed idlers, a SWIR peak power of 45 W was obtained. In this configuration the power conversion from pump to idler peak was 23 % [7]. However such performance was obtained with a pump peak power of 360 W, a level impossible and impractical to reach in CW regime. Moreover as a duty cycle of 1/1100 was applied on the pump, the repetition rate of the SWIR pulsed output may not be suited for some application.

In the present letter, we introduce a SWIR all-fiber source design featuring a high power (from 15 dBm to more than 25 dBm) CW output. The source is based on the conversion of an O-band signal (1260 nm to 1360 nm) to a SWIR idler via four-wave mixing (FWM) in a fiber optic parametric amplifier (FOPA) and on the idler's subsequent amplification in a Thulium doped fiber (TDF). Both amplification stages are pumped by the same C-band laser, leading to a power transfer from the pump to the amplified idler as high as 25 %, which is larger than for existing SWIR CW sources purely based on parametric amplification [5]. To the best of our knowledge, a setup making use of parametric amplification assisted by a Thulium doped medium around 2 µm has only previously been reported in a resonant configuration [8], thus lacking the mode-hop free tuning capability.

2. Operating principle and experimental setup

The wavelength conversion and amplification architecture reported in this section is based on a FOPA followed by a Thulium doped fiber amplifier (TDFA) whose main role is to amplify the SWIR idler previously generated in the FOPA. Due to the relatively low conversion efficiency from the O-band signal to a SWIR band idler, the FOPA operates in the un-depleted pump regime leading to a high unused pump power at its output. The corresponding idler gain equation for a FOPA operating in this regime is reported in [6]. Contrarily, in the TDFA a high fraction of the pump power is transferred toward the idler and SWIR spontaneous emission. In addition to amplification in the SWIR band, the TDF section strongly absorbs in the O-band such that the second section of the source also performs a useful preliminary filtering of the unwanted wavelengths, namely the O-band signal and the C-band pump [8]. The schematic of the proposed scheme is shown in Fig. 1.

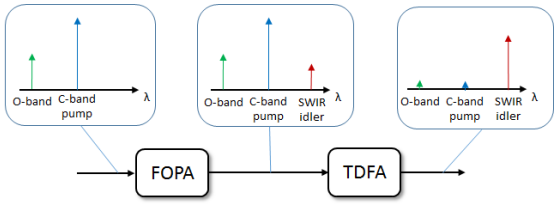

Fig 1. Schematic of the architecture showing generation, amplification and attenuation undergone by the three waves.

The FOPA section consists of a CW pump from an external cavity laser (ECL) at 1565.6 nm, phase-modulated with a pseudo-random binary sequence (PRBS) to suppress stimulated Brillouin scattering (SBS), and amplified by a high power Erbium doped fiber amplifier (EDFA). A power of 34.5 dBm is obtained after filtering of the amplified stimulated emission (ASE) by a tunable band pass filter (TBF). The SBS return losses were monitored through a circulator and kept below 0 dBm. A second ECL tunable over the O-band provides the signal wave. The signal is amplified by a semiconductor optical amplifier (SOA) to 16 dBm and coupled with the pump through a 1310/1550 nm wavelength multiplexer (MUX1). Both waves are then directed to 350 m of a highly nonlinear fiber (HNLF) such that a CW idler is generated via FWM. Depending on the O-band signal wavelength, the idler is generated between 1850 nm and 2070 nm. The corresponding experimental setup is shown in Fig. 2.

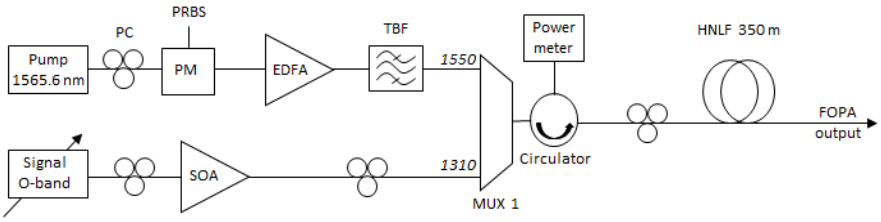

Fig. 2. Experimental setup for SWIR light generation: PC: Polarization controller, PM: Phase modulator, PRBS: Pseudo-random binary sequence, SOA: Semiconductor optical amplifier, EDFA: Erbium-doped fiber amplifier, TBF: Tunable band pass filter, MUX1: 1310/1550 nm wavelength multiplexer, HNLF: Highly nonlinear fiber.

The zero dispersion wavelength (ZDW), third and fourth order dispersion terms at the ZDW (β_3 and β_4, respectively) and the nonlinear coefficient γ of the HNLF were characterized with the method presented in [9] which consists of injecting a Watt-level CW pump near the ZDW and recording the frequency detuning between the modulation instability (MI) peaks and the pump. The measured MI detuning as a function of pump wavelength is plotted in Fig. 3(a). By fitting the detuning presented in Fig. 3(a), we estimated an average ZDW at 1569.05 nm, $\beta_3 = 4.6 \cdot 10^{-2}$ ps^3/km, $\beta_4 = -2.9 \cdot 10^{-5}$ ps^4/km and $\gamma = 14$ W^{-1}.km^{-1}. Clear MI peaks were not observed for a pump near the ZDW or in the normal dispersion regime, which could be attributed to strong dispersion fluctuations, leading to uncertainties in assessing the value of β_4. However by exploiting the anomalous regime pumping detuning, we can assert that the average value of β_4 should be close to the one given above. This negative value enables in theory normal regime pumping of the HNLF for efficient narrow band generation with reduced amplified parametric noise [10]. The theoretical CE (idler power at the output of the HNLF divided by signal power at its input) calculated using the fitting values for a 34.5 dBm pump at 1565.6 nm (normal dispersion) is shown in Fig. 3(b). The result predicts a targeted conversion between a 1320 nm signal and a 1930 nm idler as well as a gain bandwidth (CE > 0 dB) of about 4 nm.

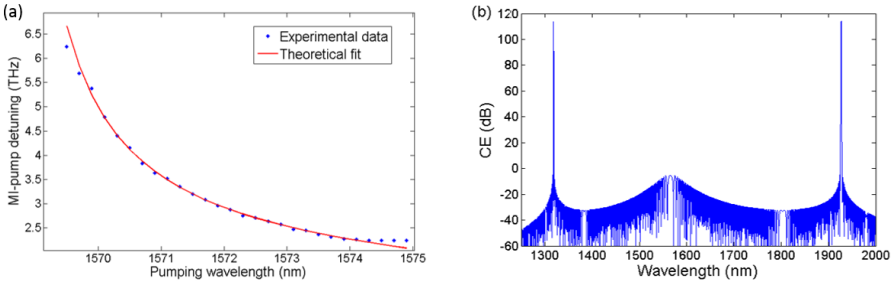

Fig. 3. (a) Frequency detuning between the pump and the MI peaks as a function of the pump wavelength. Blue squares: experimental data. Red line: the detuning computed with the parameters sought after. (b) Theoretical CE corresponding to the retrieved parameters and a 34.5 dBm pump at 1565.6 nm.

Two different assemblies of TDFs, based on commercially available Thulium fibers, were appended at the output of the HNLF, as shown in Fig. 4. The absorption cross section of the used fiber spans over all the L-band and is well suited for amplification of a signal around 1.95 µm [11]. The first configuration (Fig. 4(a)) consists of a 50 cm or 4.5 m long TDF section directly spliced at the output of the HNLF. The amount of pump energy transferred to the idler via Tm^{3+} ions depends on the TDF length, thus enabling control over the gain undergone by the idler wave. In the second configuration (Fig. 4(b)), the idler is first separated from the pump by a 1600/1960 nm coupler, and sent through 4.5 m piece of TDF. The idler is then recombined with the pump and both waves are coupled into an 11.5 m piece of TDF. With such configuration, the TDFA is expected to efficiently amplify longer wavelengths in the SWIR range as backscattered ASE from the 11.5 m piece of TDF will pump the 4.5 m segment [12, 13].

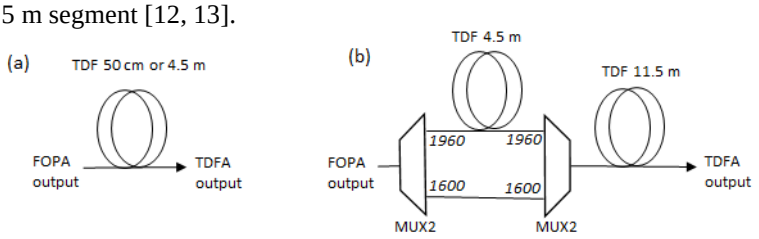

Fig. 4. Amplifier configuration with one Thulium fiber piece (a) and two fiber pieces (b). TDF: Thulium doped fiber, MUX2: 1600/1960 nm wavelength multiplexer.

3. Results and discussions

The FOPA stage was experimentally characterized by sweeping the signal wavelength over the O-band and observing the spectrum obtained at the HNLF output on the optical spectrum analyzer (OSA). As for all spectra presented in this section, a 20 dB C-band attenuator was used before the OSA. The absorption function of this attenuator was measured from 1.25 µm to 2.1 µm with a custom supercontinuum source. While the attenuation value reaches the stated 20 dB in both the O-and C-band, attenuation drops to 13.5 dB at 1950 nm. The attenuation characteristic of this element was subsequently taken into account when calculating CEs and output powers. The superimposed FOPA's output spectra are displayed in Fig. 5(a) as observed on the OSA, while the corresponding CE is shown in Fig. 5(b).

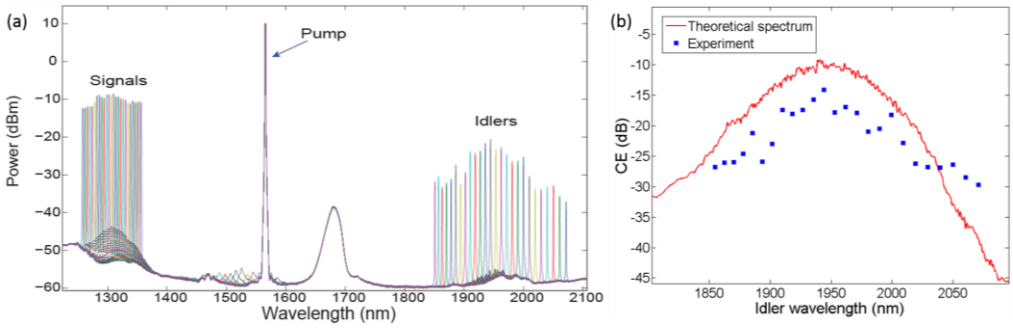

Fig. 5. (a) Superimposed spectra at the output of the HNLF stage for different O-band signals and a pump at 1565.6 nm (resolution: 1 nm). (b) Experimental (blue squares) and theoretical (red line) CE as a function of the idler wavelength. Random variations of the ZDW were taken into account for the theoretical fit.

A remarkably clean conversion from the O-band to SWIR is obtained, leveraging normal pumping regime with negative β_4 which strongly reduces the parametric amplified noise. A maximum CE of -15 dB is achieved for an idler near 1950 nm with a 3 dB bandwidth close to 80 nm. Idlers up to 2071 nm were generated, limited by the tunable range of the O-band source. Due to this relatively low CE, the pump is not depleted and we measured 32 dBm of remaining power at 1565.6 nm at the output of the HNLF. This unused power will subsequently be used for pumping of the TDF. The maximum CW idler power of -5 dBm is

located at 1945 nm. The parametric bandwidth measured (Fig. 5) is clearly broader than expected, and its amplitude is much lower than the theoretical value. The broadening and CE reduction can both be in part attributed to the random variations of the ZDW along the propagation distance [10, 14]. To illustrate this phenomenon we computed the CE theoretical spectrum according to the discrete model described in [15]. We assumed a ZDW standard deviation of 0.6 nm, a correlation length of 6 m and we averaged the spectra over 100 different ZDW distributions. Average dispersion properties of the fiber are kept the same, and attenuation is taken into account. We used pump properties identical to the ones in the experiment. The obtained simulation results illustrate the broadening of the CE bandwidth as well as a strong reduction in the CE value when random fluctuations of the ZDW are taken into account. A discrepancy of about 5 dB between the measured CE and simulated CE values is still observed, which can attributed to other factors such as random birefringence [16].

After the characterization of the FOPA, the first configuration of the TDFA was tested. A 50 cm long piece of TDF was directly appended to the FOPA and spectral measurements were performed. The spectra for various signal wavelengths are displayed on Fig. 6(a). The gain on the idler in this stage reaches 27 dB around 1.9 µm as shown in Fig. 6(b), and the maximum obtained output power reaches 15 dBm CW at 1936 nm. Some spontaneous lasing was observed on the amplified Raman peak around 1.68 µm. This effect appears at wavelengths where the net gain is high in the overall setup and is attributed to undesired feedback effects. The triangular peaks from 1.4 µm to 1.6 µm are measurement artifacts due to the large SWIR power sent into the OSA. Due to the wavelength conversion nature of the source, multiple O-band signals can be simultaneously converted to the SWIR and subsequently amplified. Fig. 6(c) shows the simultaneous generation of two SWIR seeds when two O-band signals were coupled through a 50/50 tap at the input of the FOPA. One of the signals was fixed to 1311 nm while the second one was swept between 1353 and 1293 nm. As expected, the FOPA + TDFA configuration enables simultaneous generation and amplification of two (or multiple) SWIR idlers.

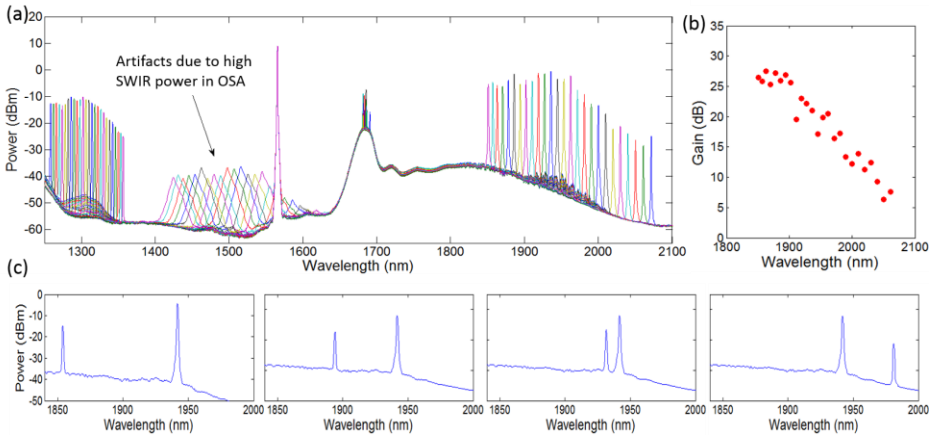

Fig. 6. (a) Superimposed spectra for different O-band signals recorded at the output of 50 cm TDF (resolution: 1 nm) and (b) Calculated gain experienced by the SWIR signal in the TDFA; (c) Optical spectra at the output of the 50 cm TDF when two signals are simultaneously converted (resolution: 1 nm). One signal was maintained at 1311 nm while the second signal was tuned to 1353, 1333, 1315 and 1293 nm (left to right).

The previous configurations allows us to tune the SWIR source over all the available FOPA band but the pump is only weakly absorbed (about 1 dB lost in TDF), leading to a large unused pump power. For better pump utilization, we increased the TDF length to 4.5 m and recorded the spectra (Fig. 7(a)). This configuration allows for the generation of amplified idlers from 1867 nm to 1958 nm with a 4 dB ripple. The pump is totally absorbed in the TDF, amplifying the SWIR waves with high quantum efficiency to powers up to 28.5 dBm CW at 1940 nm. As 34.5 dBm of C-band pump is injected in the FOPA, we obtain a pump-to-idler power conversion of 25 % at this wavelength. The optical signal to noise ratio (OSNR) ranges

from 25 dB at 1867 nm, to 40 dB at 1940 nm. Some broadening is observed on the idler due to the phase dithering of the pump which was optimized to enable the maximum power transfer through the HNLF. The output power also shows a ripple smaller than 3 dB over the whole tuning range. This tuning range is limited by the spontaneous lasing effect appearing when the idler is generated far from the top of Thulium emission cross section. In this case the idler does not compete enough for gain with the ASE generated in TDF, enabling the random feedbacks in the process to produce unstable lasing waves. We also tested the simultaneous conversion of multiple signals in this configuration. We coupled two and three signals to the FOPA and recorded spectra at the output of the source. The results displayed in Fig. 7(b), clearly show conversion and high power amplification of all coupled signals. Note that the difference in power in the SWIR is mainly due to the difference in power of the O-band signals. In this configuration, the generated power near 1.9 μm was high enough to engender four-wave mixing between the SWIR waves.

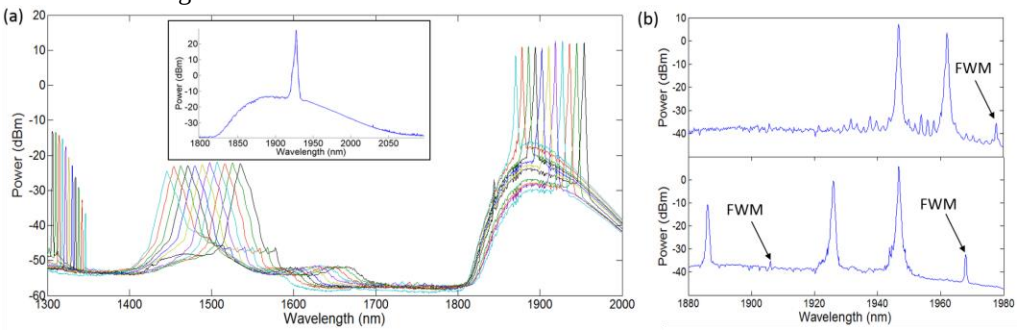

Fig. 7. Superimposed spectra for different O-band signals recorded at the output of 4.5 m TDF. Inset: zoom on the idler generated around 1930 nm with a numerical correction on the power taking the attenuator into account (resolution: 1 nm). (b) Output spectrum for a two-signals input (top) and three-signals input (bottom) (resolution: 0.5 nm).

We finally characterized the second TDFA configurations (Fig. 4b). The dual stage TDFA was investigated in order to efficiently amplify beyond 1958 nm. The obtained results are displayed in Fig. 8. The source in this configuration is tunable from 1935 nm to 1980 nm with a very flat output CW power of about 21 dBm with less than 0.5 dB fluctuations. As expected the gain in the dual stage TDFA is slightly red-shifted. The pump is totally absorbed while the O-band signals are also strongly attenuated such that only the wanted amplified SWIR signal is present at the output of the source. The OSNR is larger than 30 dB over the entire considered band. Compared to the single TDF configuration, some pump/idler power is lost in the MUX-DEMUX process, resulting in a pumping level of about 30 dBm at the input of the 11.5 m piece. The SWIR output amplitude is therefore lower than for a 4.5 m TDF only but the source emits without spontaneous lasing at longer wavelengths.

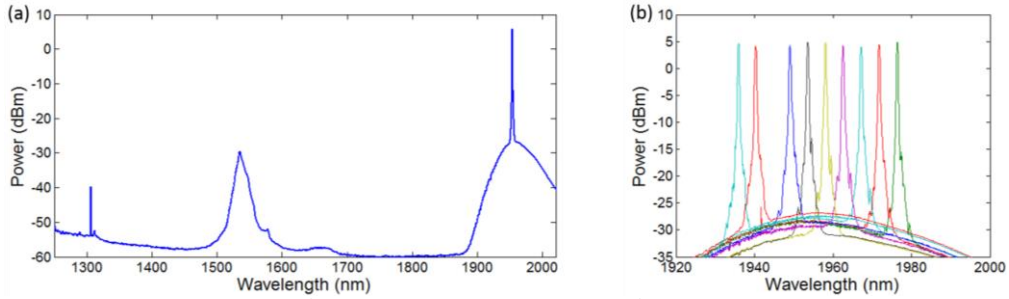

Fig. 8. (a) Spectrum at the output of the 4.5 m and 11.5 m TDF assembly for a single input signal: O-band signal and pump are absorbed in the Thulium (resolution: 1 nm). (b) Superimposed spectra at the TDF assembly output for multiple input signals (resolution: 0.5 nm). High power and low ripple is obtained between 1935 nm and 1980 nm.

4. Conclusion

An integrated combination of a parametric amplifier and Thulium-doped fiber amplifier that outputs a large CW power in the SWIR band has been demonstrated. We have investigated different configurations of the source. A widely tunable one covering more than 250 nm can be obtained with a short segment of Thulium fiber (50 cm), albeit with lower powers and high ripple. By increasing the Thulium fiber length, the obtainable power can reach up to 28 dBm with 4 dB ripple over more than 80 nm, a power level that is clearly higher than for previously reported CW and tunable SWIR sources. Finally, a two stage Thulium design can be used to amplify wavelengths between 1935 nm to 1980 nm to 21 dBm of CW power with only 0.5 dB fluctuations. Moreover, we have shown that the source can convert two or more O-band signals toward the SWIR. The ability of parametric converters to replicate O-band 10 Gb/s intensity modulated signals to the SWIR band in spite of a pump phase dithering has been previously reported [17], which shows that the architecture presented in this letter is potentially able to convert and amplify several wavelength division multiplexed channels generated in the second telecom window. For more advanced modulation schemes as well as to obtain a narrower linewidth at the idler, other techniques leveraging fiber piecewise straining of strain-insensitive fiber [5] to replace the pump phase modulation can be envisioned [6] and will be the purpose of further work.

Acknowledgment

This work is supported by the European Research Council under grant agreement ERC-2012-StG 306630-MATISSE and the SNSF under grant agreement 200021_140816. The authors would like to thank Sumitomo Electric Industries for providing the HNLF.